Original Article

Respiration-Induced Intraorgan Deformation of the Liver: Implications for Treatment Planning in Patients Treated With Fiducial Tracking

Anna K. Paulsson, MD[1], Sue S. Yom, MD, PhD[1],
Mekhail Anwar, MD, PhD[1], Dilini Pinnaduwage, PhD[1],
Atchar Sudhyadhom, PhD[1], Alexander R. Gottschalk, MD, PhD[1],
Albert J. Chang, MD, PhD[1], and Martina Descovich, PhD[1]

Abstract

Stereotactic body radiation therapy is a well-tolerated modality for the treatment of primary and metastatic liver lesions, and fiducials are often used as surrogates for tumor tracking during treatment. We evaluated respiratory-induced liver deformation by measuring the rigidity of the fiducial configuration during the breathing cycle. Seventeen patients, with 18 distinct treatment courses, were treated with stereotactic body radiosurgery using multiple fiducials. Liver deformation was empirically quantified by measuring the intrafiducial distances at different phases of respiration. Data points were collected at the 0%, 50%, and 100% inspiration points, and the distance between each pair of fiducials was measured at the 3 phases. The rigid body error was calculated as the maximum difference in the intrafiducial distances. Liver disease was calculated with Child-Pugh score using laboratory values within 3 months of initiation of treatment. A peripheral fiducial was defined as within 1.5 cm of the liver edge, and all other fiducials were classified as central. For 5 patients with only peripheral fiducials, the fiducial configuration had more deformation (average maximum rigid body error 7.11 mm, range: 1.89-11.35 mm) when compared to patients with both central and peripheral and central fiducials only (average maximum rigid body error 3.36 mm, range: 0.5-9.09 mm, $P = .037$). The largest rigid body errors (11.3 and 10.6 mm) were in 2 patients with Child-Pugh class A liver disease and multiple peripheral fiducials. The liver experiences internal deformation, and the fiducial configuration should not be assumed to act as a static structure. We observed greater deformation at the periphery than at the center of the liver. In our small data set, we were not able to identify cirrhosis, which is associated with greater rigidity of the liver, as predictive for deformation. Treatment planning based only on fiducial localization must take potential intraorgan deformation into account.

Keywords

stereotactic, liver, fiducial, deformation, radiosurgery

Abbreviations

CBCT, cone beam computed tomography; HCC, hepatocellular carcinoma; PTV, planning target volume; RBE, rigid body error; RBE_{max}, maximum rigid body error; RBE_{mean}, mean rigid body error; RBE_{CK}, dynamic fiducial rigid body error; SBRT, stereotactic body radiation therapy; 2-D, 2-dimensional; 3-D, 3-dimensional; 4-DCT, 4-dimensional computed tomography

Introduction

Stereotactic body radiation treatment is a well-tolerated conformal modality for the treatment of both primary and metastatic liver lesions. However, with highly conformal high-dose treatment, accurately targeting the lesion during free-breathing

[1] Department of Radiation Oncology, University of California, San Francisco, San Francisco, CA, USA

Corresponding Author:
Sue S. Yom, MD, PhD, Department of Radiation Oncology, University of California, San Francisco, San Francisco, CA 94143, USA.
Email: yoms@radonc.ucsf.edu

treatment poses important clinical and technical considerations. One method to account for respiration-induced tumor motion is to place gold fiducials within the liver to dynamically track the lesion during treatment.[1] Due to potential morbidity, such as tumor hemorrhage or seeding along the implantation track, fiducials are often placed adjacent to and not directly inside the target tumor. Sometimes, due to these logistical complications, a single fiducial may be used even in the presence of multiple target lesions.

Fiducial placement external to the tumor target is used to guide radiation targeting, assuming that the configuration of the fiducial relative to the tumor moves as a rigid body, without internal deformation, and that the distance from the tumor to the fiducial will remain constant. Multiple prior reports have quantified the craniocaudal movement of the liver within the abdominal cavity, which has been reported as up to 5.5 cm during maximum ventilation and 2.5 cm during normal ventilation.[2,3] Cardiac-induced motion of the liver has also been described and is mainly found in the area underneath the heart and therefore affects a relatively smaller portion of the liver. Maximum displacement of the healthy liver secondary to cardiac-induced motion ranges from 3 to 5 mm.[4] In a recent study, Xu et al evaluated rigid and nonrigid motion of liver lesions using intratreatment locations of the fiducial markers reconstructed from 2-dimensional (2-D) orthogonal images.[5] Using orthogonal X-ray data collected from a robotic stereotactic tracking system, they were able to characterize relative volume shifts as treatment progressed due to radiation-induced edema at the target. They also found that there were small intrafractional fiducial displacements due to deformation, although they did not focus on the influence that inherent liver characteristics or fiducial location impart on intrafiducial deformation. Park et al investigated the motion characteristics of the liver by extracting the coordinates of 3 fiducial markers from the X-ray projections of the cone beam computed tomography (CBCT) scans.[6] They observed a large variation in liver motion both interfractionally and intrafractionally, as well as the presence of deformation within different locations of the liver. Finally, Rohlfing et al created a 4-dimensional (4-D) model of the liver using healthy volunteers to biomechanically examine rigid and nonrigid transformation of the liver. They observed that nonrigid transformation, or deformation, of up to 34 mm can occur, indicating that the expected location of a liver region was more than 3 cm away from where it was predicted to be with rigid deformation.[7]

Understanding the factors influencing internal deformation of the liver is particularly important for defining the target volumes in image-guided liver stereotactic body radiation therapy (SBRT). Currently, there are no guidelines on how to expand planning target margins, if fiducials are placed nearby and not directly within the tumor. Using the same margins for different fiducial-to-tumor distances assumes implicitly that the fiducial-liver configuration is static. Our purpose was to quantify the intraorgan deformation of a configuration comprised of multiple fiducials. In an exploratory analysis, deformation was categorized as a function of liver disease (healthy vs cirrhotic) and fiducial location (central vs peripheral).

Materials and Methods

Seventeen patients, with 18 distinct SBRT courses delivered between 2011 and 2016 in the Department of Radiation Oncology at the University of California, San Francisco, were included in the study. One patient had an additional treatment course that required new fiducials and a separate plan.

All individuals included in this study gave informed consent for treatment, and retrospective record review for research purposes was approved by the institutional review board of the University of California. These patients all had multiple gold fiducials[2-4] implanted within the liver to guide dynamic tracking during treatment. The fiducials were placed in or near the target liver lesion by the interventional radiologist implanting the gold fiducial; degree of proximity to the lesion was achieved based on what was deemed to be a safe approach for placement. The implantation procedure was performed at least 1 week prior to the simulation to allow time for fiducial settlement, thereby minimizing the occurrence of fiducial migration. During the simulation, an 8-phase 4-D computed tomography (4-DCT) scan was obtained to evaluate target motion characteristics. All patients were treated on a robotic stereotactic treatment system (CyberKnife robotic radiosurgery system; Accuray Inc, Sunnyvale, California) using 6 MV X-rays and dynamically imaged fiducial tracking.[8] Real-time tumor motion tracking on the CyberKnife system is based on a correlation model between the position of the internal fiducial (extracted from 2-D orthogonal images) and the position of external surrogate markers (3 light-emitting diodes [LED] placed on the patient's chest prior to each treatment session, whose position is read out by an infrared camera). Prior to turning the beam on, the correlation model is created by fitting the 3-dimensional (3-D) coordinates of the fiducials with the corresponding time-stamped LED coordinates. During treatments, new X-ray images are acquired every 60 to 120 seconds and are used to update the model. Based on the model, the robot is redirected in real time to the anticipated target location so that radiation delivery is always synchronized to the continuously changing target position.

Patients were treated with doses of 1250 to 5400 cGy over 3 to 5 fractions based on the size of the liver lesion and extent of the underlying liver disease. Patients had between 1 and 4 intrahepatic lesions treated. The extent of liver disease was calculated using the Child-Pugh score for cirrhosis mortality based on laboratory values drawn within 3 months of initiation of treatment. In this study, Child-Pugh score was used as a surrogate for liver stiffness, which may impact organ deformation.

The 4-DCT was imported into an image management software (MIM; MIM Software Inc, Cleveland, Ohio). Point contours were placed at the center of each fiducial on the axial, coronal, and sagittal plane, and the 3-D coordinates of the fiducial were recorded. These points were used as a reference point from which the intrafiducial distance was calculated. Data points were collected at the 0%, 50%, and 100% inspiration phases of the respiratory cycle. These 3 sets of data points
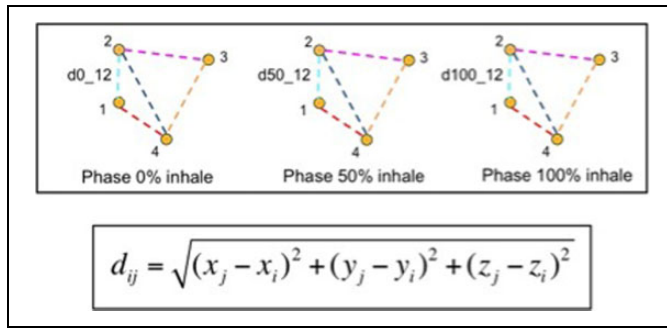
Figure 1. Rigid body error calculation. Data points were collected at the 0%, 50%, and 100% inspiration phases of the respiratory cycle, and the distance between each pair of fiducials (d_{ij}) was measured at each phase. Differences in d_{ij} between phases were used to quantify deformation in the fiducial configuration during respiration.

were selected as they represented the smallest and largest excursions of the fiducial during the respiratory cycle. The distance between each pair of fiducials (d_{ij}) was measured at each phase (Figure 1).

Differences in d_{ij} between phases were calculated and used to quantify deformation in the fiducial configuration during respiration. The maximum rigid body error (RBE_{max}) was calculated as the largest difference in the intrafiducial distances between the 2 respiratory phases:

$$RBE_{max} = \max(|d_{ij}^0 - d_{ij}^{50}|, \ |d_{ij}^0 - d_{ij}^{100}|, \ |d_{ij}^{50} - d_{ij}^{100}|).$$

The mean rigid body error (RBE_{mean}) was calculated as the average difference in the intrafiducial distances between the 2 respiratory phases:

$$RBE_{mean} = \left(\frac{\text{mean}|d_{ij}^0 - d_{ij}^{50}| + \text{mean}|d_{ij}^0 - d_{ij}^{100}| + \ \text{mean}|d_{ij}^{50} - d_{ij}^{100}|}{3} \right).$$

For each pair of fiducials (i, j), the average deformation was defined as the average difference in intrafiducial distances over the 3 respiratory phases:

$$\text{Average deformation} = \left(\frac{|d_{ij}^0 - d_{ij}^{50}| + |d_{ij}^0 - d_{ij}^{100}| + \ |d_{ij}^{50} - d_{ij}^{100}|}{3} \right).$$

We used a threshold of 2 mm as a cutoff to define the occurrence of clinically significant deformation. For treatments conducted with dynamic fiducial tracking, the dynamic fiducial rigid body error (RBE_{CK}) is defined as the maximum difference in the intrafiducial distances between the digitally reconstructed radiograph (DRR) and the X-ray images obtained during treatment:

$$RBE_{CK} = \max(|d_{12}^{DRR} - d_{12}^{X-ray}|, \ |d_{23}^{DRR} - d_{23}^{X-ray}|, \\ |d_{13}^{DRR} - d_{13}^{X-ray}|).$$

For robotic stereotactic treatments at our institution, the error threshold is set to 2 to 2.5 mm. Depending on target margins and other clinical consideration, the RBE_{CK} threshold

is set to be more or less stringent. Murphy[9] calculated the fiducial-based tracking accuracy as a function of perturbation of the fiducial configuration, and their data can be used to select the RBE threshold. If the tracking error is above this threshold, an interlock results and the treatment is paused. For this analysis, a cutoff was set at 2 mm to define a clinically significant deformation.

A peripheral lesion was defined by a location within 1.5 cm of the liver edge, and all other lesions were characterized as central lesions. The 1.5 cm cutoff was determined by measuring the closest distance from the center of each fiducial to the liver capsule; the median of those values was 1.5 cm. Values equal to or less than 1.5 cm from the liver edge defined peripheral fiducials, and values greater than 1.5 cm defined central fiducials.

Results

Eleven patients had primary hepatocellular carcinoma (HCC) and 6 had metastatic disease. For metastatic tumors, the primary disease histologies included colorectal carcinoma, esophageal carcinoma, breast adenocarcinoma, and base of tongue squamous cell carcinoma. Ten patients had Child-Pugh class A liver disease, 4 had class B, 3 had class C, and 1 had insufficient laboratory data for calculation (metastatic breast cancer). Five patients had centrally located fiducials, 5 had peripheral fiducials, and 8 had both peripheral and central fiducials. For a complete description of patient characteristics and rigid body error results, see Table 1.

For 5 patients with only peripherally located fiducials, the average RBE_{max} was 7.11 mm (range: 1.89-11.35 mm), and for those with peripheral and central or only centrally located fiducials, the average RBE_{max} was 3.36 mm (range: range: 0.5-9.09 mm), which did represent a significant difference in deformation ($P = .037$). The RBE_{max} and RBE_{mean} for all patients are presented in Table 2 for peripheral fiducials only and central/peripheral and central fiducials. Although there was a significant difference in the deformation, with only 5 patients in the peripheral-only fiducial cohort, we recognize that our study is limited by its small size. The largest excursions were 11.3 mm (Figure 2) and 10.6 mm, both found in patients with only peripheral fiducials. In the patient in Figure 2, the very large deformation (11.3 mm) between the 0% and the 100% phase was attributable to compression of the liver due to increased thoracoabdominal pressure in maximal respiration.

Across all of the patients, for each fiducial pair, we examined the potential correlation of intrafiducial distance with absolute deformation averaged among the 3 respiratory phases (Figure 3). Although the largest deformation (10.6 mm) was observed for an intrafiducial separation of 10.1 cm (peripherally located fiducials), the data showed a poor linear correlation ($R^2 = .019$), indicating that the location of the fiducials was more important than the distance between them. The lack of correlation between intrafiducial distance and average deformation could have also been influenced by the limited number of patients.

Table 1. Patient Characteristics.

Patient ID	Number of Liver Lesions	Number of Fiducials	Fiducial Location	Type of Lesion	Child-Pugh Class
1	1	3	Central	Colorectal	A
2	1	3	Central	HCC	A
3	1	3	Peripheral (1), central (2), peripheral (3)	HCC	A
4	1	3	Central	HCC	C
5	2	3	Central	HCC	C
6	2	3	Central (1,3), peripheral (2)	HCC	A
7	2	2	Peripheral	Base of tongue	A
8	3	2	Peripheral	Breast	Undetermined
9	4	4	Peripheral	HCC	A
10	2	2	Peripheral (1), central (2)	HCC	B
11	1	2	Central (1), peripheral (2)	HCC	C
12	2	2	Peripheral	HCC	B
13	4	4	Peripheral	HCC	B
14	3	3	Peripheral (1), central (2,3)	HCC	B
15	3	3	Peripheral (1) central (2)	Colorectal	A
16	1	2	Central	Colorectal	A
17	1	3	Peripheral (1,3), central (2)	Esophageal	A
18[a]	2	4	Central (1, 2) peripheral (3, 4)	Base of tongue	A

Abbreviations: HCC, hepatocellular carcinoma; SBRT, stereotactic body radiation therapy.
[a]Patient 18 had additional metastatic disease noted in the liver and was treated with a second course of SBRT after additional fiducials were placed.

Table 2. RBE_{max} and RBE_{mean} for Peripheral Fiducials and for Central and Peripheral/Central Fiducials.

Patient ID	Fiducial Location	Max RBE	Mean RBE
Peripheral fiducials			
7	Peripheral	11.3	7.6
8	Peripheral	3.1	2.0
9	Peripheral	10.6	3.4
12	Peripheral	1.9	1.3
13	Peripheral	8.7	1.7
Average RBE		7.11	3.2
Central and peripheral/central fiducials			
1	Central	1.6	0.4
2	Central	1.8	0.9
3	Peripheral (1), central (2), peripheral (3)	4.5	2.6
4	Central	4.0	2.6
5	Central	5.2	3.5
6	Central (1, 3) peripheral (2)	1.9	0.8
10	Peripheral (1), central (2)	2.5	1.7
11	Central (1), peripheral (2)	0.5	0.3
14	Peripheral (1), central (2, 3)	7.3	2.9
15	Peripheral (1), central (2)	3.0	2.0
16	Central	0.5	0.3
17	Peripheral (1, 3), central (2)	9.1	4.3
18[a]	Central (1, 2), peripheral (3, 4)	1.5	0.4
Average RBE		3.36	1.75

Abbreviations: RBE, rigid body error; RBE_{max}, maximum rigid body error; RBE_{mean}, mean rigid body error.
[a]Patient 18 had additional metastatic disease noted in the liver and was treated with a second course of SBRT after additional fiducials were placed.
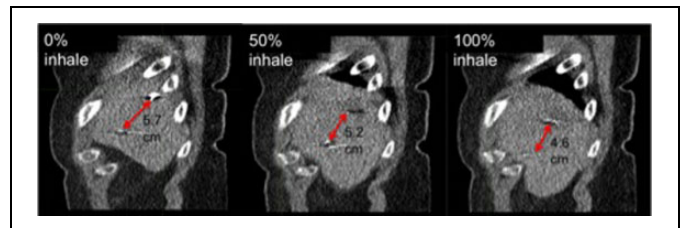
Figure 2. Four-dimensional computed tomography (4-DCT) demonstrating greatest fiducial excursion during respiration. Sagittal view from 0%, 50%, and 100% inspiration phases of the 4-DCT in a patient with liver metastases. Intrafiducial distance at the 0% phase is 5.7 cm, at 50% inspiration is 5.2 cm, and at 100% is 4.6 cm. Rigid body error calculated using the relative position of the 2 fiducials for the 0% to 50% phase is 2.6 mm, for the 0% to 100% phase is 11.3 mm, and for the 50% to 100% phase is 8.7 mm.

We did not find an overall association between deformation and liver function at the time of radiation treatment ($P = 0.88$). Patients with Child-Pugh class A disease had an average RBE_{max} of 4.6 mm (range 0.5-11.3 mm) and patients with class B and C disease had an average RBEmax of 4.3 mm (range 0.5-8.7 mm) (Figure 4).

Discussion

While the impact on the liver due to respiratory and cardiac motion has been described previously, our study describes the potential limitation of radiation treatment planning using fiducial tracking alone given the extent of intraorgan deformation of the liver inferred from the position of surrogate fiducials
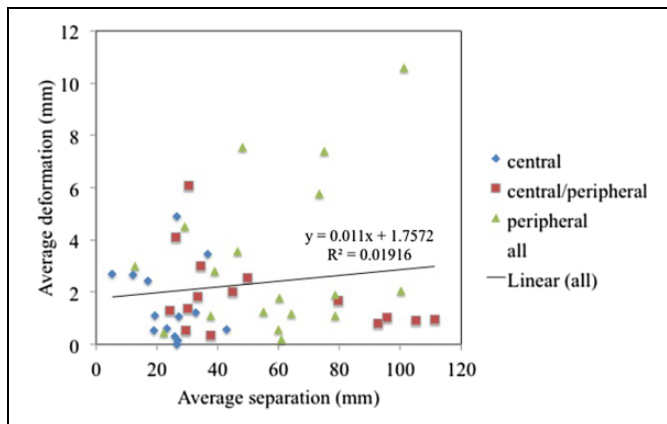
Figure 3. For each fiducial pair, we examined the potential correlation of intrafiducial distance with absolute deformation averaged among the 3 respiratory phases. Poor linear correlation ($R^2 = .019$) indicates that the location of the fiducials was more important than the distance between them.
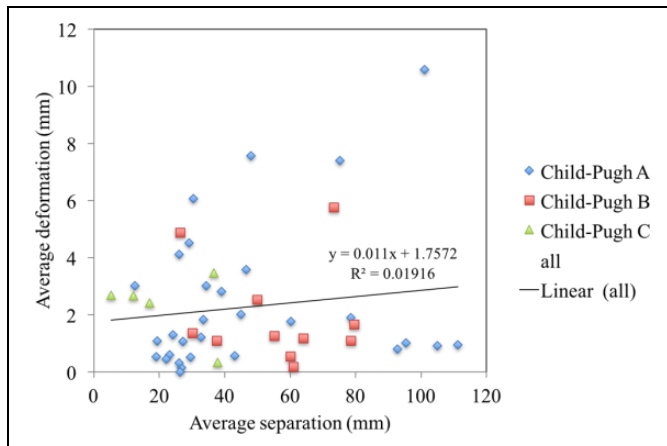
Figure 4. We examined the potential association between deformation and liver stiffness as characterized by Child-Pugh class. Poor linear correlation ($R^2 = .019$) was found, indicating a lack of association in this data set.

extracted from 4-DCT data. Original to our study is also the characterization of deformation as a function of fiducial location and disease status. Intraorgan deformation appears to be more pronounced along the periphery of the organ, while the central portion of the liver remains more rigid. This is due to the proximity of the peripheral edges of the liver to other intraabdominal and intrathoracic organs that physically compress the periphery of the liver and enact effects on local circulatory mechanics. Although the excursions of the liver throughout the respiratory cycle are easily visible on imaging, localized forms of intraorgan deformation secondary to cardiac movement, intrahepatic blood flow, and gastrointestinal peristalsis are more difficult to visualize and quantify.

In a study analyzing data collected from a robotic stereotactic tracking system, Xu et al calculated proportional volume changes throughout treatment and rotational displacement of

each fiducial relative to its mean position.[5] They were able to find that compared to the first fraction, the second and third fractions exhibited increased volumes, which could be due to radiation-induced edema. Treatment-related edema could certainly enact greater fiducial displacement as treatment progresses, especially given that stereotactic radiotherapy delivers larger fractional doses and can result in more peritumoral edema.[10] Xu et al found mean intrafractional shifts of 2.1, 2.9, and 6.4 mm in the x, y, and z planes, respectively, and mean rotational angle variations were $1.2°$, $1.8°$, and $1.7°$ in the roll, pitch, and yaw angles, respectively. The greatest displacements were seen in the superior–inferior direction and the smallest in the left–right direction. Additionally, Bertholet et al recently described a superior–inferior fiducial marker translation of up to 9.2 mm, a mean rotational range of $2.9°$ to $4.0°$ around all axes and rotation up to $28.6°$ in a single CBCT scan.[11] Although the methods used for data collection and measurement were very different from ours, with a focus on intrafractional changes rather than intrinsic temporal deformation, these data support our overall conclusion that the liver does experience multiple vectors of deformation and treatment planning processes would ideally not depend on it being an internally nondeforming organ.

In a separate study, we evaluated respiratory-induced liver rotations and their corresponding dosimetric impact.[12] We separately coregistered the planning CT with 4 phases of the 4-DCT scan by (1) rigid registration of the spine and (2) rigid registration of the 3 fiducials. For each registration, rotational and translational vectors as well as dosimetric parameters were calculated. We concluded that liver rotation had a significant impact on the dose delivered to the nearby critical structures with dose differences of 1.63, 0.5, 2.29, and 1.6 Gy on average in the maximum dose to duodenum, stomach, bowel, and esophagus, respectively.[12] This separate work confirms that motions of the liver during radiotherapy could have a meaningful clinical impact on nearby structures.

Other previous studies have shown that geometric uncertainty due to deformation and breathing variations can lead to significant deviation in the accumulated delivered dose relative to the planned dose distribution or even the dose distribution predicted using 4-DCT.[13] Deviation from the planned dose due to organ deformations can lead to exceeding the planned dose for normal tissues, particularly the bowel, which lies directly adjacent to the liver and is frequently dosed to near-maximal tolerance.[13] Marginal misses or underdosing of the target tumor could also occur if target motion is not synchronous with fiducial motions and tracking accuracy is compromised due to deformations in the fiducial configuration. As discussed earlier, this is of clinical relevance, as the fiducial is often placed near, but not within, the target, and stereotactic treatment planning margins can be very tight, especially in the periphery in adjacency to critical organs but also where intrafiducial displacements are the largest. Adjustment of planning target volume (PTV) margins requires patient-specific analysis to offset the uncertainty related to these intrafiducial deformations. We conclude from our study that intrafiducial deformation should be

of particular concern when targeting tumors lying within 1.5 cm of the periphery of the liver. As a preventive measure, at institutions that utilize fiducial tracking, it would be useful to develop internal guidelines for fiducial placement emphasizing implantation toward the central aspects of the liver, where deformation will be less, or at least to attempt to avoid placement within 1.5 cm of the periphery when possible.

In an exploratory analysis, we were unable to find a correlation between the degree of cirrhotic liver disease and intrafiducial deformation. Although Child-Pugh score was not developed as a score of liver fibrosis or stiffness, multiple prior studies, including Recio et al, have documented that liver stiffness correlates with Child-Pugh score in patients with cirrhosis and that with progressive cirrhosis there is less deformation of the liver.[14] Furthermore, recent magnetic resonance imaging and ultrasound studies have shown that with progressive cirrhosis, the deformation of the liver is less pronounced.[4,15] However, within our small study, we could not confirm these hypotheses. Additionally, although the majority of patients who have HCC have underlying cirrhosis, noncirrhotic HCC can occur, and therefore we could not assume that the patients with HCC in our study had cirrhotic livers. Hepatocellular carcinoma is frequently a diagnosis made on imaging, and histopathology documenting HCC or cirrhosis was absent in many of our patients. Nonetheless, we believe that intrafiducial deformation in patients with differing degrees of liver stiffness due to disease may be an area for further investigation.

One important limitation of this study, due to the nature of the data acquisition, was the inability to evaluate inter- or intrafraction motion of the entire fiducial configuration, as only the relative position of the fiducials used for tracking was recorded. CyberKnife patients are not aligned based on a treatment isocenter and do not have in-room volumetric imaging from which this information would be extracted.

In this study, we show that peripherally located fiducials within the liver were more subject to intraorgan deformation. We did find a significant difference between groups even with a small number of patients in this study, but further validation would be confirmatory. Although we believe that patient-specific deformation should be considered as a factor in PTV margin adjustment, additional studies would provide more capacity to create robust deformation models and better quantify recommended margin expansions. Gating according to a specific phase of the respiratory cycle would be a potential solution, if this technology were used in conjunction with confirmation of the reproducibility of the fiducial configuration in the treatment phase, as assessed on 4-DCT.[6,16] In patients who are to have multiple lesions treated without gating (for instance, on CyberKnife), we recommend the creation of a separate treatment plan for each distinct lesion, as the relative position of the tumors within the liver does not remain constant during the breathing cycle. Dose accumulation may be used to combine these separate treatment plans to obtain the dose–volume histogram for the liver as a whole. Furthermore, in this scenario, when medically possible, the implantation of multiple fiducials, each immediately adjacent to or in close proximity to each lesion, is recommended, such that the deformations of the fiducial-to-tumor distance can be minimized.

Conclusion

The liver frequently experiences intraorgan deformation, and a configuration of multiple fiducials does not act as an internally static structure. In this study, we observed the greatest deformation at the periphery within 1.5 cm of the liver edge, which has important clinical implications for location-specific planning margin adjustment. This finding holds particular relevance for lesions at the inferior liver edge, which often abut bowel, and where unanticipated deformation may place the bowel in a high-dose region. Further studies are planned to define population-based margins based on lesion location and the distance of the tumor target from the fiducial used for tracking.

References

1. Hoogeman M, Prevost JB, Nuyttens J, Poll J, Levendag P, Heijmen B. Clinical accuracy of the respiratory tumor tracking system of the cyberknife: assessment by analysis of log files. *Int J Radiat Oncol Biol Phys*. 2009;74(1):297-303.

2. Balter JM, Ten Haken RK, Lawrence TS, Lam KL, Robertson JM. Uncertainties in CT-based radiation therapy treatment planning associated with patient breathing. *Int J Radiat Oncol Biol Phys*. 1996;36(1):167-174.

3. Suramo I, Paivansalo M, Myllyla V. Cranio-caudal movements of the liver, pancreas and kidneys in respiration. *Acta Radiol Diagn (Stockh)*. 1984;25(2):129-131.

4. Chung S, Kim KE, Park MS, Bhagavatula S, Babb J, Axel L. Liver stiffness assessment with tagged MRI of cardiac-induced liver motion in cirrhosis patients. *J Magn Reson Imaging*. 2014; 39(5):1301-1307.

5. Xu Q, Hanna G, Grimm G, et al. Quantifying rigid and nonrigid motion of liver tumors during stereotactic body radiation therapy. *Int J Radiat Oncol Biol Phys*. 2014;90(1):94-101.

6. Park J, Park S, Kim J, et al. Liver motion during cone beam computed tomography guided stereotactic body radiation therapy. *Med Phys*. 2012;39(10):6431-6442.

7. Rohlfing T, Maurer CR, O'Dell WG, Zhong J. Modeling liver motion and deformation during the respiratory cycle using intensity-based nonrigid registration of gated MR images. *Med Phys*. 2004;31(3):427-432.

8. Dieterich S, Gibbs IC. *The CyberKnife in Clinical Use: Current Roles, Future Expectations, in IMRT, IGRT, SBRT—Advances in*

the Treatment Planning and Delivery of Radiotherapy. Basel, CH: Karger; 2011.

9. Murphy MJ. Fiducial-based targeting accuracy for external-beam radiotherapy. *Med Phys*. 2002;29(3):334-344.

10. Timmerman R, Kavanagh B. Stereotactic body radiation therapy. *Curr Probl Cancer*. 2005;29(3):120-157.

11. Bertholet J, Worm ES, Fledelius W, Hoyer M, Poulsen PR. Time-resolved intrafraction target translations and rotations during stereotactic liver radiation therapy: implications for marker-based localization accuracy. *Int J Radiat Oncol Biol Phys*. 2015;95(2):802-809.

12. Pinnaduwage DS, Paulsson A, Sudhyadhom A, et al. Dosimetric impact of liver rotations in stereotactic body radiation therapy. *Med Phys*. 2015;42(6):3303.

13. Velec M, Moseley JL, Craig T, Dawson LA, Brock KK. Accumulated dose in liver stereotactic body radiotherapy: positioning, breathing and deformation effects. *Int J Radiat Oncol Biol Phys*. 2012;83(4):1132-1140.

14. Recio E, Macias J, Rivero-Juarez A, et al. Liver stiffness correlates with Child-Pugh-Turcotte and MELD scores in HIV/hepatitis C virus-coinfected patients with cirrhosis. *Liver Int*. 2012;32(6):1031-1032.

15. Zaleska-Dorobisz U, Kaczorowski K, Pawlus A, Puchalska A, Inglot M. Ultrasound elastography—review of techniques and its clinical applications. *Adv Clin Exp Med*. 2014;23(4):645-655.

16. Poulsen P, Worm E, Hansen R, Larsen L, Grau C, Hoyer M. Respiratory gating based on internal electromagnetic motion monitoring during stereotactic liver radiation therapy: first results. *Acta Oncol*. 2015;54(9):1445-1452.